Materials Views
www.MaterialsViews.com

ADVANCED FUNCTIONAL MATERIALS
www.afm-journal.de

FULL PAPER

Plasticization of PEDOT:PSS by Common Additives for Mechanically Robust Organic Solar Cells and Wearable Sensors

*Suchol Savagatrup, Esther Chan, Sandro M. Renteria-Garcia, Adam D. Printz, Aliaksandr V. Zaretski, Timothy F. O'Connor, Daniel Rodriquez, Eduardo Valle, and Darren J. Lipomi**

Despite the ubiquity of poly(3,4-ethylenedioxythiophene):poly(styrenesulfonate) (PEDOT:PSS) in applications demanding mechanical flexibility, the effect on the mechanical properties of common additives—i.e., dimethylsulfoxide (DMSO), Zonyl fluorosurfactant (Zonyl), and poly(ethyleneimine) (PEI)—has not been reported. This paper describes these effects and uses plasticized films in solar cells and mechanical sensors for the detection of human motion. The tensile moduli of films spin-coated from solutions containing 0%, 5%, and 10% DMSO and 0.1%, 1%, and 10% Zonyl (nine samples total) are measured using the buckling technique, and the ductility is inferred from measurements of the strain at which cracks form on elastic substrates. Elasticity and ductility are maximized in films deposited from solutions containing 5% DMSO and 10% Zonyl, but the conductivity is greatest for samples containing 0.1% Zonyl. These experiments reveal enlargement of presumably PEDOT-rich grains, visible by atomic force microscopy, when the amount of DMSO is increased from 0% to 5%. PEI—which is used to lower the work function of PEDOT:PSS—has a detrimental effect on the mechanical properties of the PEDOT:PSS/PEI bilayer films. Wearable electronic sensors employing PEDOT:PSS films containing 5% DMSO and 10% Zonyl are fabricated, which exhibit detectable responses at 20% strain and high mechanical robustness through elastic deformation.

1. Introduction

Poly(3,4-ethylenedioxythiophene):poly(styrenesulfonate) (PEDOT:PSS, **Figure 1**) is a polyelectrolyte complex used ubiquitously as an electrode in organic electronic and optoelectronic devices.[1] Its high conductivity[2] and transparency,[3] low sheet resistance,[4] and versatility of processing from aqueous solution[5] make it an attractive choice for transparent anodes in organic solar cells,[6] and light-emitting devices,[7] and as electrodes in organic bioelectronics.[8] It can be used either alone[6] or in concert with indium tin oxide (ITO) or transparent conductors based percolated networks of conductive nanoparticles.[9] General methods of lowering the work function of PEDOT:PSS—e.g., using thin layers of amine-containing small molecules[7,10] and polymers[11]—enable its use as the cathode for organic solar cells in all-organic devices.[12] The use of transparent electrodes as both the top and bottom contacts enable semitransparent solar cells and displays.[7] The use of polymeric top and bottom contacts, in particular, enables all-solution-processing[6] and could pave the way toward ultra-compliant—i.e., stretchable and extremely flexible—devices.[13] The use of PEDOT:PSS in flexible and stretchable electronics,[5] however, demands a rigorous characterization of its mechanical properties. While the tensile modulus of the most common formulation of PEDOT:PSS can be quite high (≥2 GPa),[14] it has also demonstrated potential value as a stretchable transparent conductor for mechanically robust, portable devices for energy[15] and biomedical applications.[8b] Additives, such as co-solvents,[16] surfactants,[4] and other polymers[11] designed to improve the processability or work function of PEDOT:PSS for a given application are also likely to change drastically the mechanical properties of the pure material.[17] Despite the necessity of additives in essentially all applications to PEDOT:PSS in flexible electronics,[12] quantification of the substantial effects of these additives on the mechanical properties has received relatively little attention,[13] though previous reports have described the mechanical properties as a function of relative humidity under strain applied parallel[18] and perpendicular to the films.[19] This paper describes the effect of dimethylsulfoxide (DMSO, added to PEDOT:PSS to increase its conductivity[12]) a flurosurfactant (Zonyl, added to increase its wettability on hydrophobic substrates[16]), and polyethyleneimine (PEI, laminated to PEDOT:PSS to alter its work function[11]) on the tensile modulus and ductility of PEDOT:PSS. We

S. Savagatrup, E. Chan, S. M. Renteria-Garcia,
A. D. Printz, A. V. Zaretski, T. F. O'Connor,
D. Rodriquez, E. Valle, Prof. D. J. Lipomi
Department of NanoEngineering
University of California
San Diego, 9500 Gilman Drive, Mail Code 0448,
La Jolla, CA 92093–0448, USA
E-mail: dlipomi@ucsd.edu

DOI: 10.1002/adfm.201401758

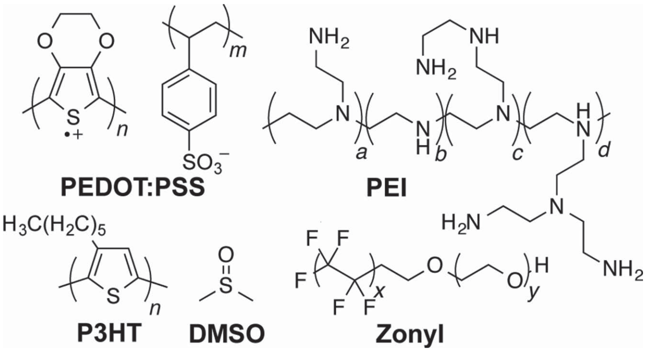

Figure 1. Chemical structures of PEDOT:PSS, PEI, P3HT, DMSO, and Zonyl.

then used these highly plasticized films to produce (1) organic solar cells using the plasticized formulation of PEDOT:PSS and (2) wearable electronic sensors exhibiting detectable responses at 20% strain and high mechanical robustness through elastic deformation.

Stretchable (i.e., elastic or ductile) electronic devices based on organic semiconductors could have applications in a wide range of fields, from energy[20] to medicine.[21] The most successful approaches to the realization of stretchable organic electronic devices have relied on directing strain away from the active components by using stretchable interconnects or buckled, wavy layouts to convert global tensile strains into local bending strain to minimize deformation.[22] Another approach is to use fractured films of organic materials that nevertheless maintain percolated pathways to the electrodes.[23] Materials that accommodate strain by virtue of their molecular or solid-state packing structures—intrinsic stretchability—could simplify processing and fabrication, and lead to better performing devices than those that rely on topographic patterns or fractured thin films.[24] Our group and others are attempting to understand the molecular and microstructural parameters that influence the mechanical properties of organic semiconductors.[25] We believe that a complete understanding of these properties will not only facilitate processing of devices for near-term applications, but could also further the development of a new form of stretchable electronics in which every component of the device accommodates the strain due to its molecular or microstructural characteristics.[24]

PEDOT:PSS is a polyelectrolyte complex prepared by the oxidative polymerization of EDOT in the presence of PSS.[1] In solution, it exists as relatively high-MW chains of PSS decorated by relatively shorter oligomers of PEDOT.[14] It is perhaps the most technologically ubiquitous conductive polymer, and is used commonly as an antistatic coating on photographic film.[26] In research laboratories, it is a component of essentially all organic solar cells and light-emitting diodes. Commercially available formulations differ primarily on the basis of the ratio of PEDOT and PSS. The formulation Clevios PH1000, manufactured by Hereaus, has a weight ratio of 1:2.5. It has achieved bulk conductivities of ≈500 S cm^{-1} when 5–7% dimethylsulfoxide (DMSO) is added as a secondary dopant.[27]

PEDOT:PSS is generally cast into films from aqueous suspension by spin-coating for laboratory-scale devices;[4] recent work has shown its amenability to spray-coating,[5] gravure printing,[16] and slot-die coating.[28] The surface tension of pure water renders as-received formulations incompatible with hydrophobic substrates.[16] Co-solvents (e.g., isopropanol)[5] or surfactants (e.g., Zonyl fluorosurfactant,[16] now called Capstone by DuPont) are generally required to coat plastic foils or organic active layers as is required in "inverted" solar cells.[16] The dramatic effects of these additives on the morphology and intermolecular forces of PEDOT:PSS—as manifested in the surface energy—suggests that the effects on the mechanical properties might be equally dramatic. These effects have not, however, been described.

The mechanical properties of pure films of PEDOT:PSS have been measured by several research groups. Measured by tensile testing of relatively thick (≥10 µm) films and fibers at 50% relative humidity, PEDOT:PSS exhibited moduli of 1.1–2.2 GPa.[18] Tahk et al. used the method based on the mechanical buckling of thin films of PEDOT:PSS films on PDMS substrates and found a similar modulus of 2.2 GPa.[14] Interestingly, the modulus was relatively insensitive to the ratio of PEDOT to PSS in the film.[14] The authors attributed this effect to the fact that the PSS component had a significantly greater molecular weight and dominated the mechanical response of the composite material.[14] Dupont and co-workers have noted that thin films of PEDOT:PSS exhibit moisture-assisted decohesion.[19] Other PEDOT-containing composites have achieved impressive combinations of elasticity and conductivity. For example, EDOT electropolymerized in a solution containing *para*-toluenesulfonate and polyurethane can form a conductive composite that can be stretched reversibly up to 50%, while maintaining a conductivity of up to 100 S cm^{-1} when stretched up to 100% strain.[29] A PEDOT:PSS-polyionic liquid blend achieved strains of 350% with an decrease in conductivity of only a factor of two at the maximum strain (but from a low initial conductivity of 10^{-3} S cm^{-1}).[30] The commercial formulation of PEDOT:PSS can also accommodate strains of up to 30% reversibly, on stretchable substrates, though smaller strains of about 10% cause the film to deform plastically; repeated strains above the onset of plastic deformation are thus accommodated by topographic buckles, as opposed to the intrinsic elasticity of the material.[17]

In addition to its role as an electrode, PEDOT:PSS has a serendipitous role as an adhesion promoter between compliant substrates and organic semiconductors. For example, our laboratory observed that the presence of the PEDOT:PSS—which has good adhesion to both UV/ozone-activated PDMS and polymer:fullerene films—significantly suppressed the formation of cracks in devices under biaxial tensile strain.[31] The importance of adhesion on suppressing the formation of cracks in compliant thin-film devices has been observed before in copper films on polyimide substrates, in which systems employing a chromium adhesion layer can accommodate strains up to 50% without cracking the copper film.[32] For film-substrate systems exhibiting poor adhesion, global strains localize in the film to delaminated regions and cause premature cracking.[33] Moreover, cracks propagate through layers, and thus the strain at which an organic electronic device fails may therefore depend entirely on the mechanical properties of the PEDOT:PSS, regardless of the elasticity or ductility of the active materials. In situations that impose stresses at the interface between layers in a device, it is often the interface between

PEDOT:PSS and the active material that fractures. Fracture energies in the range of 0.1 – 1.6 J m^{-2}, depending on the ratio of P3HT to PCBM in the active layer, have been reported by Dupont et al. for organic solar cells.[34] Factors known to weaken the adhesion of PEDOT:PSS with other layers include relative humidity, temperature, mechanical stress, and the percent incorporation of PCBM in P3HT:PCBM bulk heterojunctions.[35] Our experiments were designed to isolate other parameters and test only the effect of DMSO, Zonyl, and PEI on the elasticity and ductility of PEDOT:PSS for devices in which each component was highly stretchable.

Dimethylsulfoxide (DMSO) is added to aqueous inks containing PEDOT:PSS in weight percentages of 5–10% in essentially all applications. The role of polar "secondary dopants" such as DMSO, ethylene glycol, and sorbitol is to increase the conductivity significantly, from a native conductivity of <1 S cm^{-1} to conductivities approaching 10^3 S cm^{-1}.[4] The effect of these secondary dopants is attributed to the enlargement and coalescence of conductive grains of PEDOT in the solid film upon drying at elevated temperature, which produces large regions of uninterrupted pathways for charge carriers to traverse the film.[36] While it is not believed that DMSO persists in films after drying (e.g., on a hotplate), and thus cannot behave as a plasticizer, differences in microstructure produced by different processing conditions could easily lead to large differences in the mechanical properties of thin polymeric films.[37]

Zonyl is a fluorosurfactant comprising a poly(tetrafluoroethylene) segment and a poly(ethylene oxide) segment (Figure 1). When added to commercial formulations of PEDOT:PSS in concentrations as low as 0.01–0.1%, Zonyl permits wetting of hydrophobic substrates. It is widely used to improve the wetting behavior in roll-to-roll production, especially given the inability of unmodified PEDOT:PSS formulations to wet organic active layers in organic solar cells with the inverted architecture.[16] Zonyl was also found to have the additional advantage of improving the conductivity of PEDOT:PSS beyond what is possible with DMSO alone—i.e., as a "tertiary dopant."[4] The rationale for this improvement was similar to that of the improvement brought about by DMSO, namely a coalescing of conductive grains of PEDOT within an insulating, continuous phase of PSS, as supported by atomic force microscope (AFM) images.[4] The conductivity was maximized for films cast from solutions containing 5% DMSO and 0.01–0.1% Zonyl. In addition to improved wetting behavior and conductivity, an incidental observation noted in an earlier publication suggests that Zonyl may also behave as a plasticizer.[17] In particular, for PEDOT:PSS on PDMS substrates treated with oxygen plasma, the increase in electrical resistance of films cast from solutions containing 1% Zonyl was an order of magnitude less than that of films prepared without Zonyl, when both types of films were strained by 50%.[17] Direct measurements of tensile modulus and ductility as a function of the concentration of the additive, however, were not performed.

Polyethyleneimine (PEI) was introduced by Zhou et al. as a universal method of altering the work function of electrode materials for thin-film applications.[11] In particular, a thin film of PEI changes the work function of PEDOT:PSS from 5.1 eV to 4.3 eV.[11] This addition of PEI enables the modified PEDOT:PSS to behave as the cathode and the unmodified PEDOT:PSS to behave as an anode when used together in a single cell. Our group has applied this approach to fabricate biaxially stretchable, all-polymer solar cells in order to bond them to hemispherical surfaces, but we did not examine the influence of the thin (~20 nm) PEI layer and its solvent on the mechanical properties of the PEDOT:PSS.[31] In addition, the solvent used to deposit PEI, 2-methoxyethanol (MOE), could potentially have an effect on the mechanical properties of the PEDOT:PSS films.

We measured two parameters of mechanical properties, tensile modulus and the crack on-set strain, of PEDOT:PSS films comprising different composition of DMSO and Zonyl as well as PEDOT:PSS films with a PEI layer laminated on top at constant room temperature of 23 °C and relative humidity of 50%. The tensile moduli were measured using the mechanical buckling technique originally described by Stafford et al.[38] The PEDOT:PSS films were first spin-coated on a passivated glass substrate then transferred to a PDMS substrate bearing a small pre-strain (2–4%). Release of the pre-strain produced buckling in the PEDOT:PSS films. The slope of a plot of buckling wavelength vs the thickness of the film was used to determine the tensile modulus of the film. The crack on-set strain can be used to measure the effective ductility of a film/substrate system. We measured the electrical conductivity of the films using a two-terminal measurement with silver paint as electrodes. The absence of significant contact resistance was verified using four-terminal measurements for randomly selected samples.

2. Results and Discussion

The results of the mechanical measurements are shown in **Figure 2**. Zonyl has a dramatic plasticizing effect on PEDOT:PSS, as seen in the decrease in tensile modulus (Figure 2a) and increase in crack-onset strain (Figure 2b). In each triad on the plots in which the concentration of DMSO in the ink was kept constant at 0, 5, or 10 wt%, the concentration of Zonyl dramatically increased the ductility of the film, as manifested by an increase in the crack-onset strain from ≤5% strain for all samples with 0.1% Zonyl, to up 25–40% strain for all samples coated from inks containing 10% Zonyl. These values are a factor of three greater than previous highest ductility reported in PEDOT:PSS films, which cracked at strains of 12%.[17] Ductility was highly correlated with tensile modulus (Figure 2b). An increase in Zonyl from 0.1 wt% to 1 wt% produced a decrease in the tensile moduli by a factor of two for samples with 5% and 10% DMSO, and by a factor of eight for samples with 0% DMSO. Due to the high vapor pressure of Zonyl, we expected that a significant fraction remained in the PEDOT:PSS film, and that it functioned as a typical plasticizer, i.e., by increasing the free volume in the film and weakening intermolecular forces between the polymer chains. We note that obtaining the tensile moduli of films containing 10% Zonyl by the buckling method was difficult, because the buckling technique requires that the modulus of the film be at least two orders of magnitude greater than that of the PDMS substrate.[38] We did not observe buckles for the sample spin-coated from a solution with 0% DMSO and 10% Zonyl. We believe this film simply compressed along with the PDMS

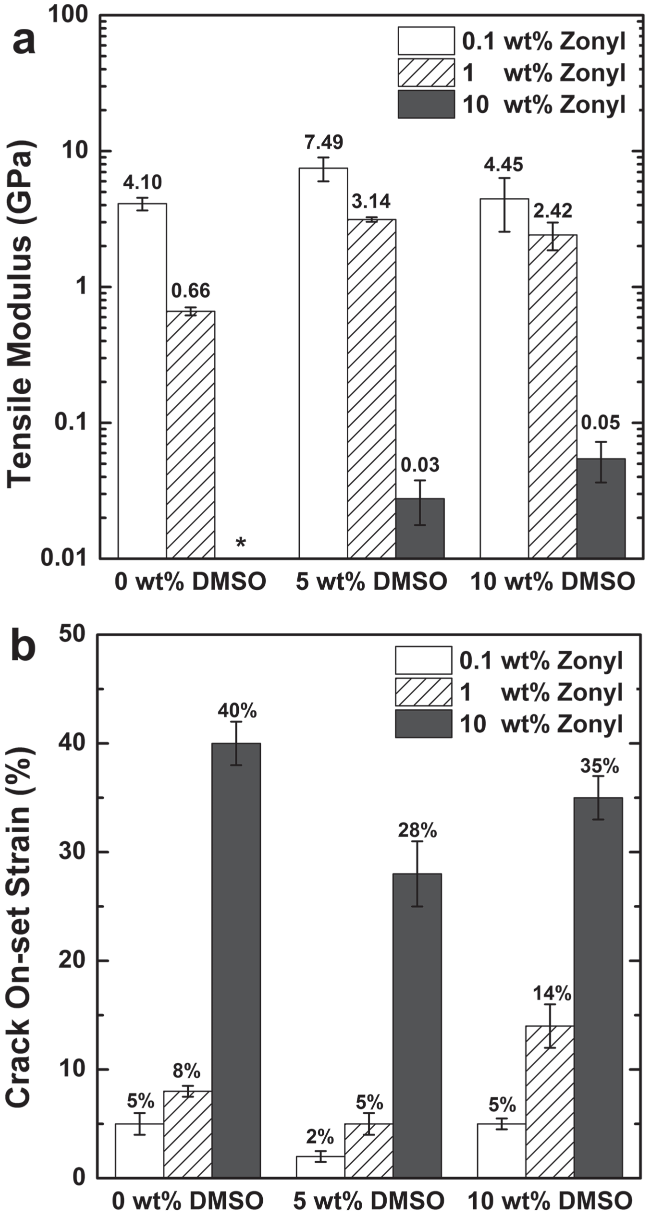

Figure 2. Mechanical properties of PEDOT:PSS films as a function of DMSO and Zonyl concentration in the ink. a) Tensile moduli obtained via the buckling methodology. The asterisk (*) refers to the absence of data from the sample coated from ink containing 0 wt% DMSO and 10 wt% Zonyl, which was too soft to measure. b) Crack-onset strains of the thin films transferred onto PDMS substrates.

substrate after release of the pre-strain, rather than formed buckles.

The data shown in Figures 2a and 2b also revealed a dependence of the mechanical properties of PEDOT:PSS on the amount of DMSO present in the ink. Films deposited from solutions containing 5% DMSO were the stiffest and least ductile, though the effect was not nearly as strong as for Zonyl. Unlike Zonyl, significant amounts of DMSO were not likely to remain in the film after drying at 100 °C on a hotplate, and thus effects produced by DMSO were attributed to changes in the microstructure of the film. The relative stiffness and brittleness of the films containing 5% DMSO mirrored the effects of DMSO on the conductivity (a topic to which we will return), which suggest that the interconnectedness of the PEDOT-rich domains in the film that are associated with the greatest conductivity also produced the greatest stiffness.

While the substantial increase in ductility of the PEDOT:PSS films could be optimized by varying the concentration of DMSO and Zonyl, we note that the mechanical properties of the solar cell devices will be dependent on all of the components and not solely on the properties of PEDOT:PSS films. Other components of the devices—the active component layer, the electrode, the substrate, and the encapsulation—may generate cracks that lead to the device failure prior to the crack-onset strain of the PEDOT:PSS films. However, for the case in which the active layer and the top electrode are more mechanically compliant than the PEDOT:PSS films, the PEDOT:PSS films had a deleterious effect on the effective ductility of the devices.[31] We also attempted to correlate the mechanical data to the conductivity as a function of both the concentrations of DMSO and Zonyl present in the aqueous solution. **Figure 3**a shows the measured sheet resistance of the PEDOT:PSS films with constant thickness of 150 nm. While the effect of DMSO on the conductivity of PEDOT:PSS has been studied exhaustively,[12] the effect of Zonyl has only been examined one other time, and with only one concentration of DMSO.[4] Our results are largely consistent with those previously reported: the sheet resistance of the films coated without DMSO were too high for most device applications (>100 kΩ sq^{-1}). Similar values of sheet resistance were obtained for inks containing both 5% and 10% DMSO, with 5% producing somewhat more conductive films (other reports suggest 7% may be the optimum value).[27] The lowest sheet resistance of 63 Ω sq^{-1} was achieved using 5% DMSO and 0.1% Zonyl. While small concentrations of Zonyl increased the conductivity (lowered the sheet resistance) of PEDOT:PSS compared to samples without Zonyl, concentration in excess of 0.1% increased the sheet resistance of the samples spin-coated from solutions containing either 5% or 10% DMSO. This result agreed well with the previous findings by Vosgueritchian et al. where Zonyl at the concentration of 0.01% and 0.1% lowered the sheet resistance of PEDOT:PSS films containing 5% DMSO when compared to PEDOT:PSS films containing 5% DMSO and no Zonyl; however, when the concentration of Zonyl increased to 1% and 10%, higher sheet resistances were obtained.[4] The conventional rationale for the improvement in conductivity with either DMSO or Zonyl is the apparent enlargement of PEDOT-rich grains within a PSS matrix, which are generally assigned on the basis of AFM; however, morphology at the surface is not necessarily representative of the microstructure of the bulk.[12]

We examined the evolution of resistance as a function of strain for PEDOT:PSS films coated from solutions containing 0.1% Zonyl and 10% Zonyl (with a constant 5% DMSO), Figure 3b. The PEDOT:PSS films were spin-coated on passivated glass then transferred to an unstrained PDMS substrate. Electrical contact was made using eutectic gallium-indium (EGaIn). The resistances of the films were then measured as a function of the linear strain applied by a computer-controlled linear actuator. As expected from the values of the respective crack-onset strain, the relative resistance (R/R_0) of the films

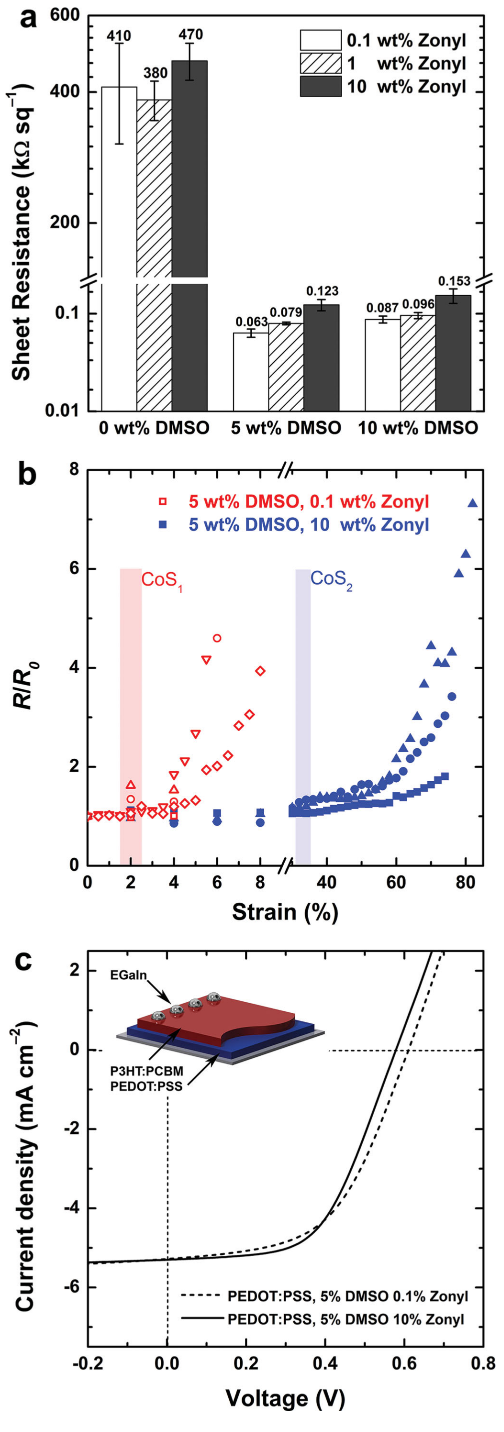

Figure 3. a) Sheet resistance as a function of both DMSO and Zonyl concentration in the ink. b) Plot of normalized resistance (R/R_0) vs strain for PEDOT:PSS films spun from 0.1% and 10% Zonyl (with constant 5% DMSO) transferred onto PDMS substrates. Shaded areas represent the crack-onset strains (CoS) of the respective films. The widths of the shaded areas are two times the standard deviations for the measurements of crack-onset strain. The different marker symbols (squares, triangles, etc.) refer to different films coated from the same solution. c) Photovoltaic properties of bulk heterojunction devices with the architecture PEDOT:PSS/P3HT:PCBM/EGaIn comprising PEDOT:PSS films spun from 0.1% and 10% Zonyl (both with 5% DMSO). Each curve represents the average of 8 devices.

spun using 0.1% Zonyl increased rapidly at relatively low strain compared to those of the films spun using 10% Zonyl. For the films containing 0.1% Zonyl, the increase in relative resistance occurred at the strain slightly greater that the crack-onset strain of 2%, and after 8% strain, the resistance of the films were greater than the sensitivity limit of our electrometer. We attributed the initial increase in resistance to the generation of minor cracks on the films and the result of increase in the particle separation when the films are stretched. The large increase in resistance thereafter to major cracks that led to the catastrophic failure of the films. We observed a much smaller increase in the relative resistance for the films with 10% Zonyl for up to ~40% strain and catastrophic failure at ~80% strain. We note that the observed relative resistance had a wider spread between samples after the films were stretched beyond the crack-onset strain. We attributed this effect to the idiosyncratic nature of the formation and propagation of cracks between samples prepared similarly. For example, a sample with a crack spanning nearly the entire width of the sample will have a much higher resistance than one with two disconnected cracks, which permit substantial conductance.

We fabricated bulk heterojunction organic photovoltaic (OPV) devices to evaluate whether the increase in the sheet resistance of the PEDOT:PSS films spun using 10% Zonyl would have a deleterious effect on the device performance when compared to films spun using 0.1% Zonyl. The sheet resistance of the transparent electrodes plays an important role in the performance of the OPV devices. High values of sheet resistance directly influence the series resistance within an OPV device; high series resistance lowers the fill factor (*FF*) and the overall power conversion efficiency (*PCE*). We compared OPV devices based on P3HT:PCBM with cell architecture of PEDOT:PSS/P3HT:PCBM/EGaIn using two different PEDOT:PSS solutions: (1) 5% DMSO, 10% Zonyl and (2) 5% DMSO, 0.1% Zonyl. We chose the solution containing 5% DMSO and 10% Zonyl because we found the composition of the films spun from this ink to be the most mechanically compliant, but which also retained adequate conductivity. The solution containing 0.1% Zonyl was used previously by our group to optimize PCE in OPV devices comprising P3AT:PCBM.[25b] Figure 3c shows that the *J–V* curves of devices using two different compositions of the PEDOT:PSS solutions were similar. The photovoltaic performances for the two configurations were constant, within experimental error, exhibiting *FF* of 54% to 56% and *PCE* of 1.7%, which agrees well with results reported earlier in literature with a similar cell architecture.[4] These results suggested that the higher sheet resistance of the solution containing 5% DMSO and 10% Zonyl had minor effects on the performance of the solar cells and could be employed in highly stretchable devices.

To attempt to correlate the microstructure of the films as apparent on the surface to the conductivity (sheet resistance), we obtained AFM phase images of samples spun from inks with all nine combinations of concentrations of DMSO and Zonyl (**Figure 4**). Samples deposited from solutions containing either 0% or 5% DMSO and 0.1% or 1% Zonyl (the top-left four images) exhibited a qualitative increase in size of the PEDOT-rich domains as visible in the phase-contrast images (from 0% to 5% DMSO). Increasing the concentration of DMSO

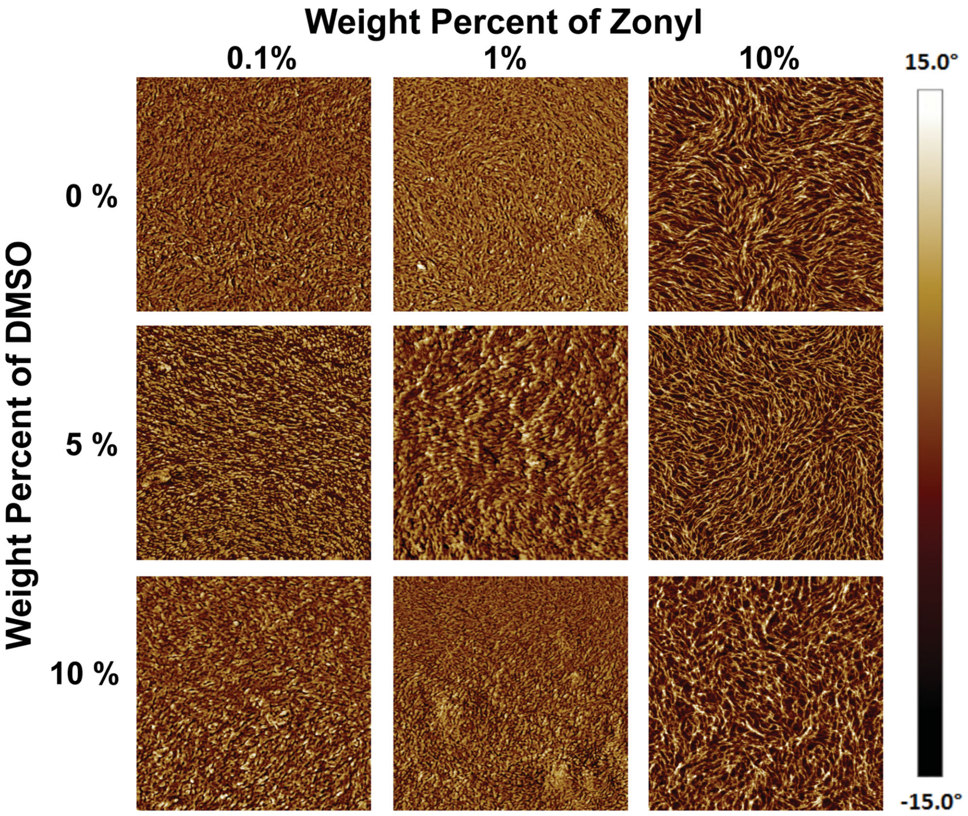

Figure 4. AFM phase images of PEDOT:PSS films as a function of the content of DMSO and Zonyl additives in the solution used for deposition. The dimensions of each AFM image are 1.5 μm × 1.5 μm.

further to 10%—again ignoring the right-hand column—decreased the sizes of these grains (which is particularly clear in the transition from 5% DMSO/1% Zonyl to 10% DMSO/1% Zonyl); this reduction in size is correlated to a decrease in conductivity, as we expected due to precedent in the literature.[12] All samples containing 10% Zonyl exhibited high-aspect-ratio fibrils at the surface whose size showed no correlation with conductivity at any concentration of DMSO; these samples did however exhibit the greatest compliance and ductility. The morphology of the surface, however, may not have been representative of the microstructure of the bulk, given the likelihood that Zonyl segregated to the surface.

Additives such as poly(ethyleneimine) (PEI) have been used to lower the work function of PEDOT:PSS.[11] Such materials are necessary to produce asymmetry in the work functions in devices in which PEDOT:PSS serves as both the anode and cathode, such that the electrons and holes drift in the proper direction. The effect of treating PEDOT:PSS with PEI on the mechanical properties has not been characterized. **Figure 5**a compares the crack-onset strains of three pure PEDOT:PSS films (i, ii, and v) and two PEDOT:PSS/PEI bilayer films (iii and iv) prepared using 5% DMSO and 10% Zonyl and stretched on PDMS substrates. Sample (i) represents the PEDOT:PSS films that were spin-coated on passivated glass and transferred to PDMS substrates; the value is duplicated from Figure 2; sample (ii) represents the films that were spin-coated directly onto PDMS substrates. The minor increase in crack-onset strain, or the apparent ductility, of films that were spin-coated directly from the films that were transferred is attributed to increased adhesion between the PEDOT:PSS films and the PDMS substrates when spin-coated directly on the PDMS. In samples represented by (iii) and (iv), a layer of PEI was deposited on the PEDOT:PSS films by spin-coating from a dilute solution of PEI in 2-methoxyethanol (MOE) after the initial drying of the PEDOT:PSS films. We observed significant decreases in the crack-onset strain with the addition of PEI layer for both transferred and directly spin-coated samples, sample (iii) and (iv) respectively. We investigated this increase in apparent brittleness by conducting a control experiment in which we treated the PEDOT:PSS films with the solution of pure MOE via the same spin-coating parameters. The further decrease in the crack-onset strain exhibited by sample (v) suggested that the MOE significantly embrittled the PEDOT:PSS films, perhaps by extracting some of the Zonyl from the films. Figure 3b shows the evolution of relative resistance as a function of tensile strain. The results correlated well with the crack-onset strains in which the films that were treated with MOE, the most brittle films, experienced a rapid increase in R/R_0 values at low strains, ~8%. Films with a thin layer of PEI showed relatively constant R/R_0 values up to 16% strain, at which point the resistance increased over the detection limit. We observed a very different trend in the sample spin-coated with PEI when compared to the other samples where the relative resistance remained relatively constant through the crack-onset strain and suddenly increased beyond the detection limit. We attributed this effect to the sudden development of large cracks in the

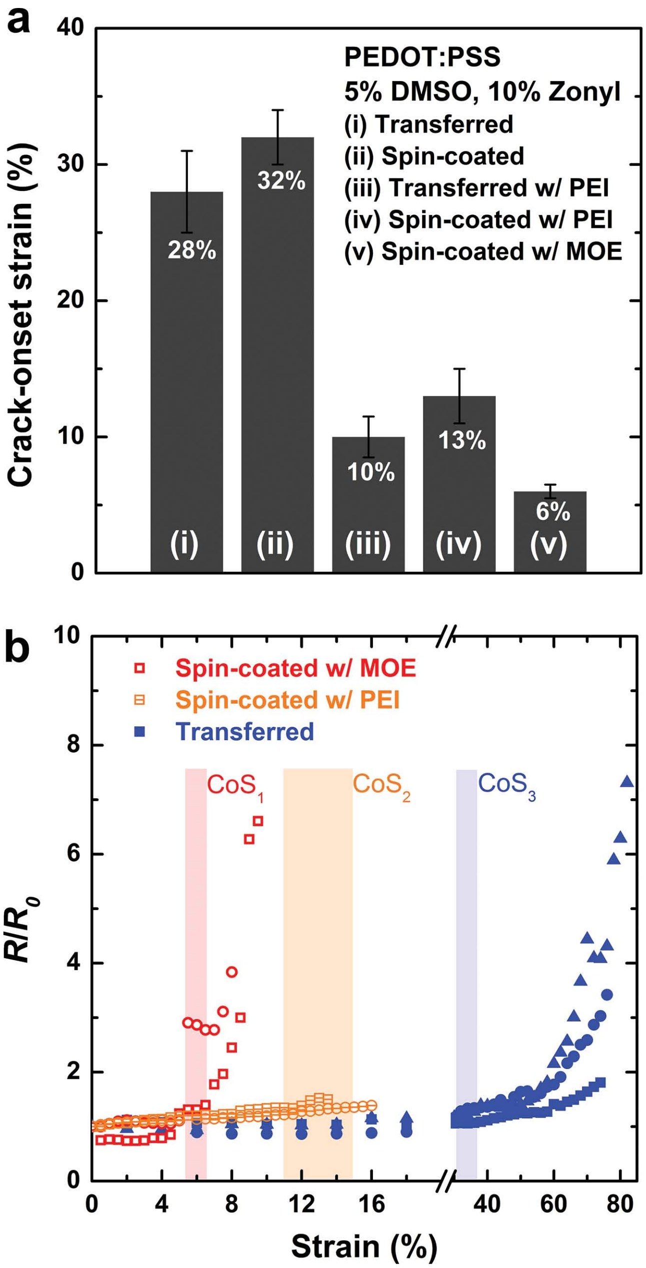

Figure 5. a) Comparison of the crack-onset strains of the PEDOT:PSS films spun using 5% DMSO and 10% Zonyl with five different treatments: neat PEDOT:PSS films (both transferred from passivated glass, (i), and directly spin-coated onto PDMS substrate, (ii), films with a layer of PEI (both transferred, (iii), and directly spin-coated, (iv), and films treated after deposition by spin-coating with neat 2-methoxyethanol, (v). b) Evolution of relative resistance as a function of strain. Shaded areas refer to the crack-onset strains of respective samples. The widths of the shaded areas correspond to two times the standard deviation of the measurements of crack-onset strain.

bilayer films rather the generation of minor cracks found in the other samples. The major cracks that spanned the whole length of the films led to the sudden failure of the devices rather than the gradual increase in the relative resistance. The increase in apparent brittleness in PEDOT:PSS films laminated with PEI or exposed to MOE solvent was an unfortunate yet important observation that should be taken into account when designing organic electronic systems requiring mechanical robustness or substantial deformation.

To demonstrate the utility of these plasticized films of PEDOT:PSS in devices, we fabricated wearable electronic sensors in which we measured the change in resistance as a function of bending strain (i.e., to signal the bending of a joint). A piezoresistive effect—i.e., a change in electrical resistivity upon the application of mechanical strain—has been described for PEDOT:PSS by Lang and co-workers.[39] The authors patterned PEDOT:PSS films on polyimide membranes using standard photolithography of photoresist and lift-off procedure and fabricated resistors with dimensions of 4 × 4 mm.[39,40] We reasoned that films of PEDOT:PSS, when plasticized by common additives (i.e., cast from inks containing 5% DMSO and 10% Zonyl), might behave as piezoresistive strain gauges for applications requiring extreme mechanical deformation (as would be required for medical prostheses and soft robotics). Unlike capacitive sensors, resistive modalities are much simpler to implement, as they are relatively unaffected by electric fields or by nearby conductors. The skin-like resistive strain sensors comprised PEDOT:PSS films that were transferred onto thin PDMS substrates and adhered to a nitrile glove using copper tape, **Figure 6**a. We selected materials for this experiment based on a finite-element analysis whose goal was to predict the maximum strain associated with the bending and unbending of the fingers, Figure 6b. The simulation accounted for the dimension of the PEDOT:PSS films and PDMS substrate and subjected them to the bending onto a 5 mm radius of curvature, approximately the radius of curvature of the second knuckle. As expected, the maximum strain occurred at the apex of the curvature with the strain of ~20%. Our analysis suggested that PEDOT:PSS films with 10% Zonyl would survive the repeated deformation of 20% strain and that the change in resistance would be measurable.

Figure 6c shows the representative result obtained from the resistive sensor placed on the nitrile glove. The measured relative resistance increased by a factor of 2–3 when the strains were applied (fingers bent). The resistance returned to the original value when the strains were removed. This behavior was sustained during cyclic loading; we tested 20 cycles. We observed instantaneous increases in R/R_0 when the strains were applied, and relatively slower decays to constant values over the period of applied strains; however, the signal to noise ratios remained relatively high throughout the experiment. We attributed the different increase in R/R_0 values among different cycles to the inability of the human hand to apply consistent strains. We note that the use of four-terminal probe will likely decrease the hysteresis in the measurement; however, the average increase in relative resistance due to the bending motion would likely remain unchanged. To control for the inconsistency of human motion, we subjected the sensors to the cycling of 0% and 20% tensile strains using a computer-controlled linear actuator (Figure 6d). Unlike the wearable sensor shown in Figures 6a and 6c, the electrodes used for the experiment shown in Figure 6d were droplets of EGaIn rather than copper tape. Given the similarity in results obtained between four-terminal measurements with brass contacts, and two-terminal measurements using EGaIn and copper

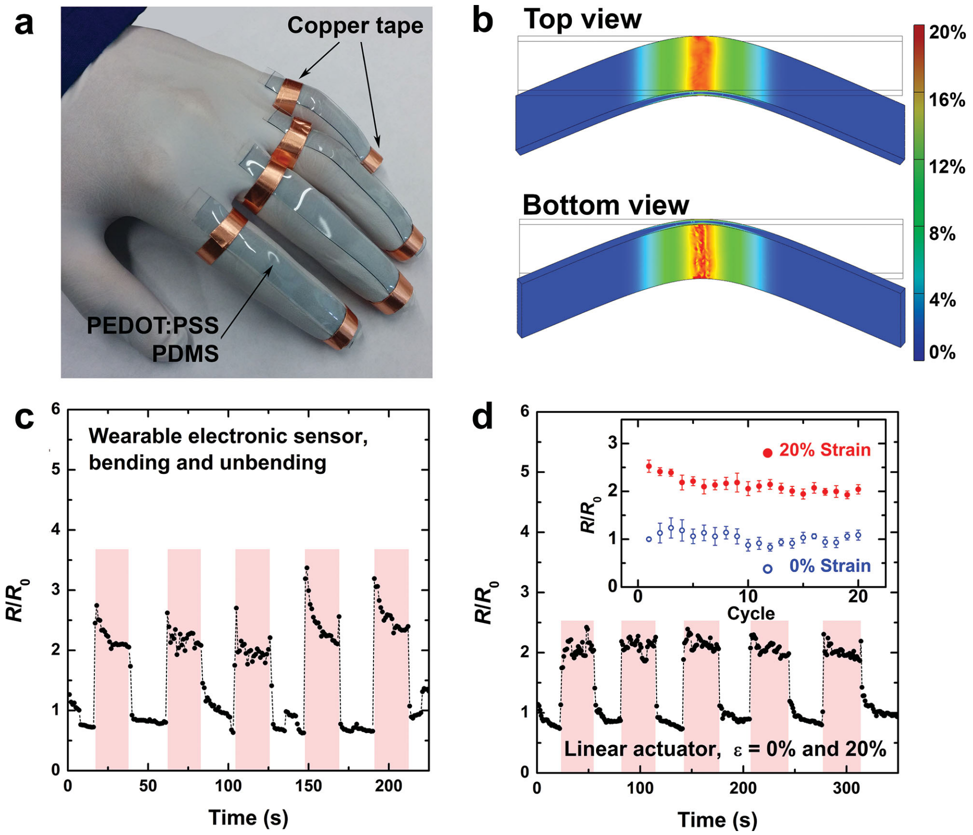

Figure 6. Images showing the characteristics of the skin-like resistive strain sensors. a) Photograph of the devices comprising PEDOT:PSS films with 5% DMSO and 10% Zonyl transferred onto thin PDMS substrates (1 mm thick) and adhered to a nitrile glove using conductive copper tape. b) Computational analysis of strain produced in the thin films when subjected to bending with the radius curvature of 5 mm, approximately the radius of curvature of the second knuckle. The peak strain occurred at the location of the second knuckle with an equivalent strain of ≈20%. c) Plot of relative resistance (R/R_0) as a function of time for the devices placed on the human hand. The shaded areas refer to when strains are applied by bending of the fingers. d) $R/R_{0\text{ vs}}$ time of the devices on the linear actuator cycling between 0% and 20% strains. The inset shows the average R/R_0 at both positions as a function of the number of cycle.

tape, we suggest an absence of substantial contact resistance. We observed a substantial reduction in noise, however, the non-instantaneous decays to the original resistance values upon relaxation remained. Such delays could be attributed to the viscoelasticity of the PDMS (the elastic regime of PDMS is approximately 10%) and the inherent properties of PEDOT:PSS. Measurements performed at the strain below the elastic limit of PDMS provided measurable change in the relative resistance; however, as shown in Figure 3b, the increase in relative resistance in that region are not sufficiently pronounced to isolate the origin of the time dependence. The inset of Figure 6d shows the cyclability of the mechanical sensor. After 20 cycles, the relative resistance of the stretched state remained constant: approximately double its value in the relaxed state.

3. Conclusions

This paper described the mechanical and electrical properties PEDOT:PSS thin films as a function of concentration of the common additives in the solution used to deposit the films. We discovered that the addition of Zonyl significantly improved the mechanical compliance, while good electrical properties (i.e., sheet resistance) were retained. The effect of the concentration of DMSO on the mechanical properties was relatively small. Our findings may provide insights toward the design of mechanically robust, highly flexible, or stretchable displays and solar cells, and resistive strain sensors for medical and robotic applications. Our experiments also highlighted a deleterious effect of incorporating PEI into all-rubber electronics; examination of the additional layer of PEI or exposure to its common solvent, MOE, revealed embrittlement of the PEDOT:PSS films. Using highly plasticized PEDOT:PSS films as resistive strain sensors could be valuable in providing electronic feedback for soft actuators in robotic applications. Understanding the role of common additives on not only the electrical properties—but also the mechanical ones—will be necessary for virtually all applications of organic semiconductors destined for stretchable, ultra-flexible, and mechanically stable applications in energy, consumer electronics, and biomedicine.

4. Experimental Section

Materials: PEDOT:PSS (Clevios PH1000) was purchased from Heraeus. The solid content of the PH 1000 solution was 1–1.3% and had a ratio of PEDOT to PSS of 1:2.5 by weight. Dimethyl sulfoxide

(DMSO) was purchased from BDH with purity of 99.9% and used as supplied. Zonyl FS-300 (Zonyl), ortho-dichlorobenzene (ODCB), poly(3-hexylthiophene) (P3HT), [6,6]-phenyl C_{61} butyric acid methyl ester (PCBM, >99%), eutectic gallium-indium (EGaIn, ≥99.99%) were purchased from Sigma-Aldrich and used as received. Polyethylenimine (PEI) was also purchased from Sigma-Aldrich and was dissolved in 2-methoxyethanol (Sigma-Aldrich) with the concentration of 1 mg mL^{-1} prior to usage. (Tridecafluoro-1,1,2,2-tetrahydrooctyl)-1-trichlorosilane (FOTS) was obtained from Gelest. PDMS (Sylgard 184, Dow Corning) was prepared according to the manufacturer's instructions at a ratio of 10:1 (base:crosslinker) and cured at room temperature for 36 to 48 hours. The dimensions of the PDMS substrates are 8 cm × 1 cm; the thickness varied depending on the experiment: 3 mm for buckling; 1.5 mm for crack-onset strain; and 1 mm for resistive strain sensors.

Preparation of PEDOT:PSS Solutions and Films: PEDOT:PSS solutions with different concentrations of DMSO and Zonyl were prepared. The PEDOT:PSS films were prepared on FOTS-passivated glass slides as the initial substrate for all experiments. Glass slides, 2.5 cm × 2.5 cm, were cleaned by bath sonication in Alconox solution, pure deionized water, acetone, and isopropanol for 10 min each. The glass slides were then treated in a plasma cleaner (30 W, 200 mtorr ambient air, 3 min) before enclosing them in a vacuum desiccator with a vial containing ca. 100 µL FOTS. The desiccator was left under dynamic vacuum for at least 12 h. The FOTS-treated glass slides were rinsed with isopropanol and dried under a stream of compressed air before use. PEDOT:PSS solutions were spin-coated directly onto FOTS-treated glass slides with spin speeds determined by the desired thicknesses. The PEDOT:PSS films were then dried on the hot plate at 100 °C for 30 min and cooled to room temperature before further testing.

Characterization of PEDOT:PSS Films: The tensile moduli of the films were measured using the buckling-based method. The PDMS substrates were prepared according to the manufacturer's instruction and cured in air at room temperature for 36–48 hours before use. We then cut the PDMS into rectangular pieces (l = 8 cm, w = 1 cm, h = 0.3 cm) and stretched to strains of 4% using a computer-controlled actuator (Newmark model ET-100–11). While the PDMS substrates were under strain, clean glass slides (5 cm × 2.5 cm, treated with FOTS to later facilitate separation of PDMS) were clipped onto the back of each PDMS substrate to maintain the strain. For each PEDOT:PSS solution, films with three different thicknesses were prepared by varying the spin speed onto separate FOTS glass slides. Transferring the PEDOT:PSS films to the pre-strained PDMS substrate was performed by initially scoring the films along the edges with a razor and placing the films against the PDMS. After applying a minimum amount of pressure to create a conformal seal between the PDMS and the PEDOT:PSS films, we separate the glass/stretched PDMS from the glass/PEDOT:PSS film in one fast motion. We used the surface of the PDMS that was cured at the air interface. We then removed the clips and allowed the PDMS to relax to the equilibrium length. Buckles formed in the PEDOT:PSS films upon relaxation of the substrates. We plotted the buckling wavelengths, λ_b, as a function of film thicknesses, d_f, then substituted the slopes of the linear fits, λ_b/d_f, and the moduli of the PDMS substrates, E_s, into Equation (1) to calculate the moduli of the PEDOT:PSS films, E_f. The Poisson's ratios of the films and the substrate, ν_f and ν_s, were assumed to be 0.35 and 0.5 respectively. In our experiment, E_s obtained were in the range of 0.6 to 0.8 MPa depending on the exact mixing ratio of base to hardener, curing time, and batch-to-batch variability.

$$E_f = 3E_s\left(\frac{1-\nu_f^2}{1-\nu_s^2}\right)\left(\frac{\lambda_b}{2\pi d_f}\right)^3 \tag{1}$$

We measured the crack-onset strain of each film by transferring PEDOT:PSS films onto unstrained PDMS substrates with thickness of 1.5 mm and stretching the substrates from 0% to 50% strains with a step size of 1% using a computer-controlled linear actuator. The thickness of all PEDOT:PSS films were kept relatively constant at ~150 nm. At each step, optical micrographs were taken to observe the film surfaces. The crack-onset strains were defined by the strain at which the first crack was observed by optical microscopy. The sheet resistance and conductivity of the films were measured by two-terminal measurements as previously described.[41] PEDOT:PSS films were prepared on FOTS-treated glass as described above; films thickness were kept constant at ≈150 nm. The absence of significant contact resistance was verified by four-terminal measurements for some samples, with good agreement in the resistance values between the two methods. AFM images were taken using tapping mode (Veeco Scanning Probe Microscope). The images were taking with the dimensions 1.5 µm × 1.5 µm. Samples used to measure the relative resistance as a function of strain were prepared in the same manner as those used to measure the crack-onset strains. The films and substrates were then mounted on the computer controlled linear actuator; electrical contacts were made using EGaIn. We measured resistance from 0% to 80% strains with a step size of 0.5% strains.

Fabrication and Characterization of OPV Devices: OPV devices were fabricated on FOTS-treated glass slides, prepared in the same manner described above. PEDOT:PSS solutions were then spin-coated onto the glass slides at 500 rpm for 4 min then 2 k rpm for 60 s. The slides were then dried on a hot plate in ambient air for 30 min; slides with PEDOT:PSS with 7% DMSO and 0.1% Zonyl were annealed at 150 °C, and slides with PEDOT:PSS with 5% DMSO and 10% Zonyl were annealed at 100 °C to avoid the formation of surface buckling. The active layer solution was prepared with a 1:1 solution of P3HT:PCBM in ODCB and stirred overnight at room temperature (40 mg mL^{-1} total solid concentration). The solution was spin-coated directly onto the PEDOT:PSS films at 500 rpm for 4 min and 2 krpm for 60 s. The films were then annealed in inert atmosphere at 125 °C for 30 min. EGaIn droplets were then applied as the top electrodes. Photovoltaic properties were measured using a solar simulator operated at AM 1.5G conditions inside a glovebox filled with nitrogen.

Acknowledgements

This work was supported by the Air Force Office of Scientific Research (AFOSR) Young Investigator Program, grant number FA9550–13–1–0156. Additional support was provided by the laboratory startup funds from the University of California, San Diego. S.S. acknowledges support provided by the National Science Foundation Graduate Research Fellowship under Grant No. DGE-1144086. A. Z. acknowledges a fellowship from SoCal Clean Energy Technology Acceleration Program from the von Liebig Center at UCSD sponsored by the US Department of Energy. E.V acknowledges support provided by the Ronald McNair Program. S. M. R.-G. acknowledges the Bridge to Engineering Success program from Tufts University.

Received: May 30, 2014
Revised: October 16, 2014
Published online: November 29, 2014

---

[1] A. Elschner, S. Kirchmeyer, W. Lovenich, U. Merker, K. Reuter, *PEDOT: Principles and Applications of an Intrinsically Conductive Polymer*, CRC Press, New York **2011**.

[2] N. Kim, S. Kee, S. H. Lee, B. H. Lee, Y. H. Kahng, Y. R. Jo, B. J. Kim, K. Lee, *Adv. Mater.* **2014**, *26*, 2268.

[3] Y. H. Kim, C. Sachse, M. L. Machala, C. May, L. Muller-Meskamp, K. Leo, *Adv. Funct. Mater.* **2011**, *21*, 1076.

[4] M. Vosgueritchian, D. J. Lipomi, Z. N. Bao, *Adv. Funct. Mater.* **2012**, *22*, 421.

[5] J. G. Tait, B. J. Worfolk, S. A. Maloney, T. C. Hauger, A. L. Elias, J. M. Buriak, K. D. Harris, *Sol. Energy Mater. Sol. Cells* **2013**, *110*, 98.

[6] Y. Galagan, E. W. C. Coenen, B. Zimmermann, L. H. Slooff, W. J. H. Verhees, S. C. Veenstra, J. M. Kroon, M. Jorgensen, F. C. Krebs, R. Andriessen, *Adv. Energy Mater.* **2014**, *4*, 1300498.

[7] F. L. E. Jakobsson, X. Crispin, L. Lindell, A. Kanciurzewska, M. Fahlman, W. R. Salaneck, M. Berggren, *Chem. Phys. Lett.* **2006**, *433*, 110.

[8] a) J. Rivnay, R. M. Owens, G. C. Malliaras, *Chem. Mater.* **2014**, *26*, 679; b) P. Leleux, J. M. Badier, J. Rivnay, C. Benar, T. Herve, P. Chauvel, G. C. Malliaras, *Adv. Healthcare Mater.* **2013**, *3*, 490.

[9] W. Gaynor, J. Y. Lee, P. Peumans, *ACS Nano* **2010**, *4*, 30; b) J. B. Wu, H. A. Becerril, Z. N. Bao, Z. F. Liu, Y. S. Chen, P. Peumans, *Appl. Phys. Lett.* **2008**, *92*, 163302.

[10] L. Lindell, A. Burquel, F. L. E. Jakobsson, V. Lemaur, M. Berggren, R. Lazzaroni, J. Cornil, W. R. Salaneck, X. Crispin, *Chem. Mater.* **2006**, *18*, 4246.

[11] Y. H. Zhou, C. Fuentes-Hernandez, J. W. Shim, J. Meyer, A. J. Giordano, H. Li, P. Winget, T. Papadopoulos, H. Cheun, J. Kim, M. Fenoll, A. Dindar, W. Haske, E. Najafabadi, T. M. Khan, H. Sojoudi, S. Barlow, S. Graham, J. L. Bredas, S. R. Marder, A. Kahn, B. Kippelen, *Science* **2012**, *336*, 327.

[12] R. Po, C. Carbonera, A. Bernardi, F. Tinti, N. Camaioni, *Sol. Energy Mater. Sol. Cells* **2012**, *100*, 97.

[13] a) D. J. Lipomi, B. C.-K. Tee, M. Vosgueritchian, Z. N. Bao, *Adv. Mater.* **2011**, *23*, 1771; b) Y. Li, Y. Masuda, Y. Iriyama, H. Okuzaki, *Trans. Mater. Res. Soc. Japan* **2012**, *37*, 303; c) Y. Li, R. Tanigawa, H. Okuzaki, *Smart Mater. Struct.* **2014**, *23*, 074010; d) C. Chen, A. Torrents, L. Kulinsky, R. D. Nelson, M. J. Madou, L. Valdevit, J. C. LaRue, *Synth. Met.* **2011**, *161*, 2259.

[14] D. Tahk, H. H. Lee, D. Y. Khang, *Macromolecules* **2009**, *42*, 7079.

[15] F. C. Krebs, T. D. Nielsen, J. Fyenbo, M. Wadstrom, M. S. Pedersen, *Energ. Environ. Sci.* **2010**, *3*, 512.

[16] M. M. Voigt, R. C. I. Mackenzie, C. P. Yau, P. Atienzar, J. Dane, P. E. Keivanidis, D. D. C. Bradley, J. Nelson, *Sol. Energy Mater. Sol. Cells* **2011**, *95*, 731.

[17] D. J. Lipomi, J. A. Lee, M. Vosgueritchian, B. C.-K. Tee, J. A. Bolander, Z. N. Bao, *Chem. Mater.* **2012**, *24*, 373.

[18] U. Lang, N. Naujoks, J. Dual, *Synthetic Met.* **2009**, *159*, 473.

[19] S. R. Dupont, F. Novoa, E. Voroshazi, R. H. Dauskardt, *Adv. Funct. Mater.* **2013**, *24*, 1325.

[20] J. Lee, J. A. Wu, M. X. Shi, J. Yoon, S. I. Park, M. Li, Z. J. Liu, Y. G. Huang, J. A. Rogers, *Adv. Mater.* **2011**, *23*, 986.

[21] a) D. H. Kim, N. S. Lu, R. Ma, Y. S. Kim, R. H. Kim, S. D. Wang, J. Wu, S. M. Won, H. Tao, A. Islam, K. J. Yu, T. I. Kim, R. Chowdhury, M. Ying, L. H. Xu, M. Li, H. J. Chung, H. Keum, M. McCormick, P. Liu, Y. W. Zhang, F. G. Omenetto, Y. Huang, T. Coleman, J. A. Rogers, *Science* **2011**, *333*, 838; b) S. Bauer, S. Bauer-Gogonea, I. Graz, M. Kaltenbrunner, C. Keplinger, R. Schwodiauer, *Adv. Mater.* **2014**, *26*, 149.

[22] a) J. A. Fan, W. H. Yeo, Y. W. Su, Y. Hattori, W. Lee, S. Y. Jung, Y. H. Zhang, Z. J. Liu, H. Y. Cheng, L. Falgout, M. Bajema, T. Coleman, D. Gregoire, R. J. Larsen, Y. G. Huang, J. A. Rogers, *Nat. Comm.* **2014**, *5*, 3266; b) M. Kaltenbrunner, T. Sekitani, J. Reeder, T. Yokota, K. Kuribara, T. Tokuhara, M. Drack, R. Schwodiauer, I. Graz, S. Bauer-Gogonea, S. Bauer, T. Someya, *Nature* **2013**, *499*, 458.

[23] A. Chortos, J. Lim, J. W. F. To, M. Vosgueritchian, T. J. Dusseault, T. H. Kim, S. W. Hwang, Z. N. Bao, *Adv. Mater.* **2014**, DOI: 10.1002/adma.201305462.

[24] S. Savagatrup, A. D. Printz, T. F. O'Connor, A. V. Zaretski, D. J. Lipomi, *Chem. Mater.* **2014**, *26*, 3028.

[25] a) S. Savagatrup, A. S. Makaram, D. J. Burke, D. J. Lipomi, *Adv. Funct. Mater.* **2014**, *24*, 1169; b) S. Savagatrup, A. D. Printz, D. Rodriquez, D. J. Lipomi, *Macromolecules* **2014**, *47*, 1981.

[26] R. C. Chiechi, J. C. Hummelen, *ACS Macro Lett.* **2012**, *1*, 1180.

[27] S. I. Na, G. Wang, S. S. Kim, T. W. Kim, S. H. Oh, B. K. Yu, T. Lee, D. Y. Kim, *J. Mater. Chem.* **2009**, *19*, 9045.

[28] N. Espinosa, M. Hosel, D. Angmo, F. C. Krebs, *Energ. Environ. Sci.* **2012**, *5*, 5117.

[29] T. S. Hansen, K. West, O. Hassager, N. B. Larsen, *Adv. Funct. Mater.* **2007**, *17*, 3069.

[30] S. J. Kwon, T. Y. Kim, B. S. Lee, T. H. Lee, J. E. Kim, K. S. Suh, *Synthetic Met.* **2010**, *160*, 1092.

[31] T. F. O'Connor, A. V. Zaretski, B. A. Shiravi, S. Savagatrup, A. D. Printz, M. I. Diaz, D. J. Lipomi, *Energy Environ. Sci.* **2014**, *7*, 370.

[32] N. S. Lu, X. Wang, Z. G. Suo, J. Vlassak, *Appl. Phys. Lett.* **2007**, *91*, 221909.

[33] D. J. Lipomi, H. Chong, M. Vosgueritchian, J. G. Mei, Z. N. Bao, *Sol. Energy Mater. Sol. Cells* **2012**, *107*, 355.

[34] S. R. Dupont, M. Oliver, F. C. Krebs, R. H. Dauskardt, *Sol. Energy Mater. Sol. Cells* **2012**, *97*, 171.

[35] V. Brand, C. Bruner, R. H. Dauskardt, *Sol. Energy Mater. Sol. Cells* **2012**, *99*, 182.

[36] X. Crispin, F. L. E. Jakobsson, A. Crispin, P. C. M. Grim, P. Andersson, A. Volodin, C. van Haesendonck, M. Van der Auweraer, W. R. Salaneck, M. Berggren, *Chem. Mater.* **2006**, *18*, 4354.

[37] O. Awartani, B. Lemanski, H. W. Ro, L. J. Richter, D. M. DeLongchamp, B. T. O'Connor, *Adv. Energy Mater.* **2013**, *3*, 399.

[38] C. M. Stafford, C. Harrison, K. L. Beers, A. Karim, E. J. Amis, M. R. Vanlandingham, H. C. Kim, W. Volksen, R. D. Miller, E. E. Simonyi, *Nat. Mater.* **2004**, *3*, 545.

[39] U. Lang, P. Rust, J. Dual, *Microelectron. Eng.* **2008**, *85*, 1050.

[40] U. Lang, P. Rust, B. Schoberle, J. Dual, *Microelectron. Eng.* **2009**, *86*, 330.

[41] A. D. Printz, E. Chan, C. Liong, R. S. Martinez, D. J. Lipomi, *PLoS One* **2013**, DOI: 10.1371/journal.pone.0083939.